



Implementation of a WENO High-Resolution Scheme

Presented By
Michael F. Harris Ph.D.
Launch Services Program, KSC

Thermal & Fluids Analysis Workshop
TFAWS 2024
August 26-30, 2024
NASA Glenn Research Center
Cleveland, OH



Introduction

- CFD at Launch Services Program
- Why use high order methods?
- Governing Equations: 2-D Euler Equations
- Immersed Boundary Method
- Moving Least Squares and Boundary Conditions
- Time Integration - SSP RK3
- Spatial Discretization – Lax-Friedrichs
- WENO Reconstruction
- Examples
 - Supersonic flow over cylinder
 - Forward facing step
 - Double Mach reflection



CFD at Launch Services Program



- Commercial CFD software used
 - StarCCM+ for general use
- NASA software used
 - Launch Ascent Vehicle Aerodynamics (LAVA)
 - Ignition overpressure and launch acoustic predictions
 - Overflow
 - External flow / aerodynamic predictions of launch vehicles
 - 6 DOF or prescribed motion simulations for booster separation
 - Fun3D
 - Vulcan
 - Hypersonic / Re-entry
 - Commercial launch vehicles are able to recover hardware
- Meshing
 - Pointwise, CGT, StarCCM+

Why use high order methods?

- Advantages
 - Higher accuracy can be achieved on a coarser mesh
 - Much better results compared to lower order schemes on a fine mesh
 - More efficient and less time consuming in that regard
- Disadvantages
 - Instabilities: High order methods like smooth solutions
 - Solution: A switch between high order and low order schemes is needed across shocks or steep gradients $f = (1 - \phi)f_{low} + \phi f_{high}$ where $0 \leq \phi \leq 1$ (TVD schemes, Limiters)
 - Complexities: Difficult to implement on irregular grids and along boundaries
 - Computational expense: Larger stencil, more computational resources
- If interested in high-speed flows and capturing thin shock waves
 - Higher accuracy is needed for effective shock capturing
 - Low order method need many grid points near the shock to resolve it
 - Grid adaption or adaptive mesh refinement (AMR)
 - Or use a higher order method such as WENO

- 2D Euler Equations for calorically perfect gas

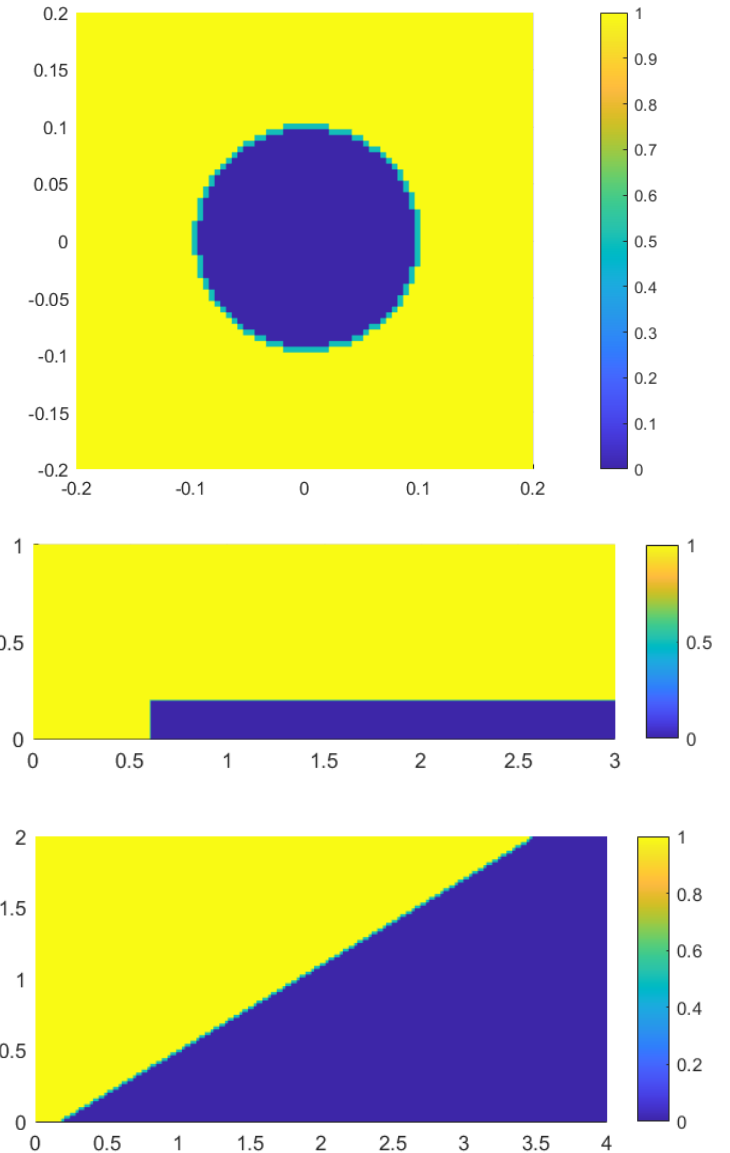
$$\frac{\partial Q}{\partial t} + \frac{\partial F(Q)}{\partial x} + \frac{\partial G(Q)}{\partial y} = 0$$

$$Q = \begin{bmatrix} \rho \\ \rho u \\ \rho v \\ \rho e_t \end{bmatrix} \quad F(Q) = \begin{bmatrix} \rho u \\ \rho u^2 + P \\ \rho uv \\ (\rho e_t + P)u \end{bmatrix} \quad G(Q) = \begin{bmatrix} \rho v \\ \rho uv \\ \rho v^2 + P \\ (\rho e_t + P)v \end{bmatrix}$$

$$e_t = e + \frac{1}{2}(u^2 + v^2) \quad e = c_v T \quad P = \rho RT$$

$$\frac{\partial Q}{\partial t} = - \left(\frac{F_{i+1/2,j} - F_{i-1/2,j}}{\Delta x} + \frac{G_{i,j+1/2} - G_{i,j-1/2}}{\Delta y} \right) = R(Q)$$

- Cartesian Mesh
 - Sharp interface immersed boundary approach
 - No inaccuracies due to high aspect ratios or skewness
 - Easy to change geometries for testing numerical methods
- Level set function is created to differentiate between fluid domain, boundary (ghost nodes), and interior grid points (blanked or solid)
- Moving Least Squares (MLS) is used to interpolate inside the fluid domain and apply boundary conditions to ghost nodes
- Inviscid flow- slip flow on walls



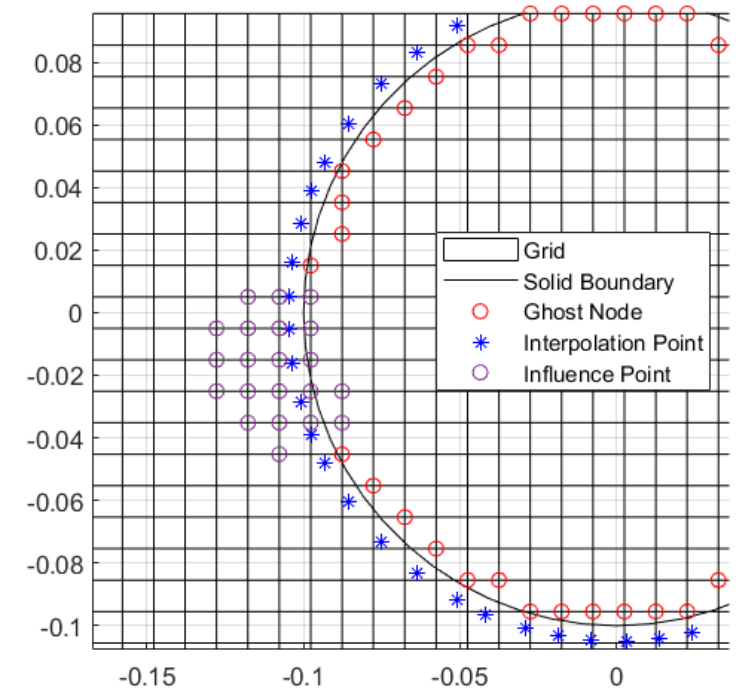
- Moving Least Squares (MLS) used to interpolate field values in the fluid region
 - For a set of chosen polynomials $P = [1, x, y]^T$ and using a sample of influence points (x, y) surrounding the interpolation point, we can approximate the field variables

$$f(x, y) = \sum_{j=1}^{NP} a_j P_j(x, y)$$

- Least squares minimization will give

$$\sum_{j=1}^{NP} a_j \left[\sum_{k=1}^{NF} P_i(x_k, y_k) P_j(x_k, y_k) \right] = \sum_{k=1}^{NF} P_i(x_k, y_k) f(x_k, y_k)$$

$$[C]_{NP, NP} \{a\}_{NP, 1} = [P]_{NP, NF} \{f\}_{NF, 1}$$



- Solving for the $\{a\}_{NP,1}$ coefficients

$$\{a\}_{NP,1} = [C]_{NP,NP}^{-1} [P]_{NP,NF} \{f\}_{NF,1}$$

- Recall

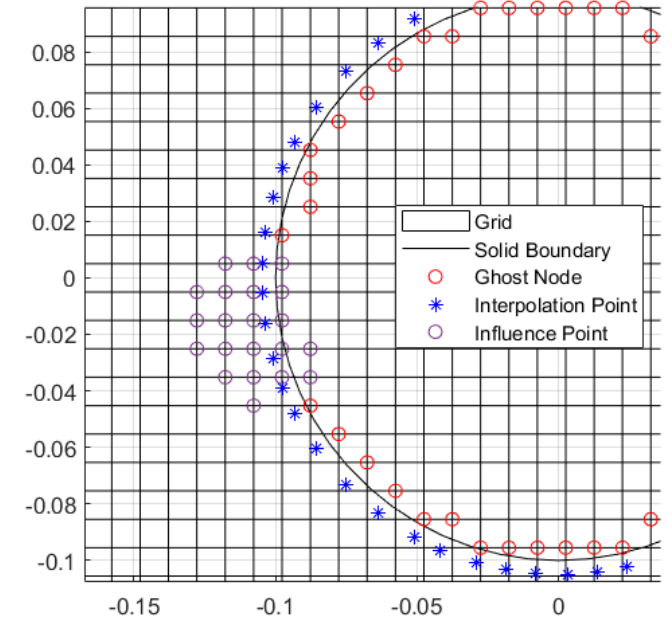
$$f(x, y) = \sum_{j=1}^{NP} a_j P_j(x, y) = \{P\}_{1,NP}^T \{a\}_{NP,1}$$

- After substitution, the field variable can be approximated by

$$f(x, y) = \{P\}_{1,NP}^T [C]_{NP,NP}^{-1} [P]_{NP,NF} \{f\}_{NF,1}$$

$$f(x, y) = \{X\}_{1,NF}^T \{f\}_{NF,1}$$

- $\{X\}_{1,NF}$ can be preprocessed, saved, and used to evaluate the field variables for each interpolation point



Update ghost nodes to enforce velocity tangent to walls or the normal velocity to zero

- Strong Stability Preserving Runge Kutta (SSP RK3) is used for time integration
- Explicit 3 stage scheme

$$\frac{\partial Q}{\partial t} = - \left(\frac{F_{i+1/2,j} - F_{i-1/2,j}}{\Delta x} + \frac{G_{i,j+1/2} - G_{i,j-1/2}}{\Delta y} \right) = R(Q)$$

$$Q_{i,j}^{(1)} = Q_{i,j}^n + \Delta t R(Q^n)$$

$$Q_{i,j}^{(2)} = \frac{3}{4} Q_{i,j}^n + \frac{1}{4} \left(Q_{i,j}^{(1)} + \Delta t R(Q^{(1)}) \right)$$

$$Q_{i,j}^{n+1} = \frac{1}{3} Q_{i,j}^n + \frac{2}{3} \left(Q_{i,j}^{(2)} + \Delta t R(Q^{(2)}) \right)$$

- Local Lax-Friedrichs / Rusanov Flux Splitting

$$\frac{\partial Q}{\partial t} = - \left(\frac{F_{i+1/2,j} - F_{i-1/2,j}}{\Delta x} + \frac{G_{i,j+1/2} - G_{i,j-1/2}}{\Delta y} \right)$$

$$F_{i+1/2,j} = \frac{1}{2} (F_{i+1/2,j}^L + F_{i+1/2,j}^R) - \frac{1}{2} S_{i+1/2,j} (Q_{i+1/2,j}^R - Q_{i+1/2,j}^L)$$

$$F_{i-1/2,j} = \frac{1}{2} (F_{i-1/2,j}^L + F_{i-1/2,j}^R) - \frac{1}{2} S_{i-1/2,j} (Q_{i-1/2,j}^R - Q_{i-1/2,j}^L)$$

$$G_{i,j+1/2} = \frac{1}{2} (G_{i,j+1/2}^L + G_{i,j+1/2}^R) - \frac{1}{2} S_{i+1/2,j} (Q_{i,j+1/2}^R - Q_{i,j+1/2}^L)$$

$$G_{i,j-1/2} = \frac{1}{2} (G_{i,j-1/2}^L + G_{i,j-1/2}^R) - \frac{1}{2} S_{i-1/2,j} (Q_{i,j-1/2}^R - Q_{i,j-1/2}^L)$$

$$S = \max(|\lambda|)$$

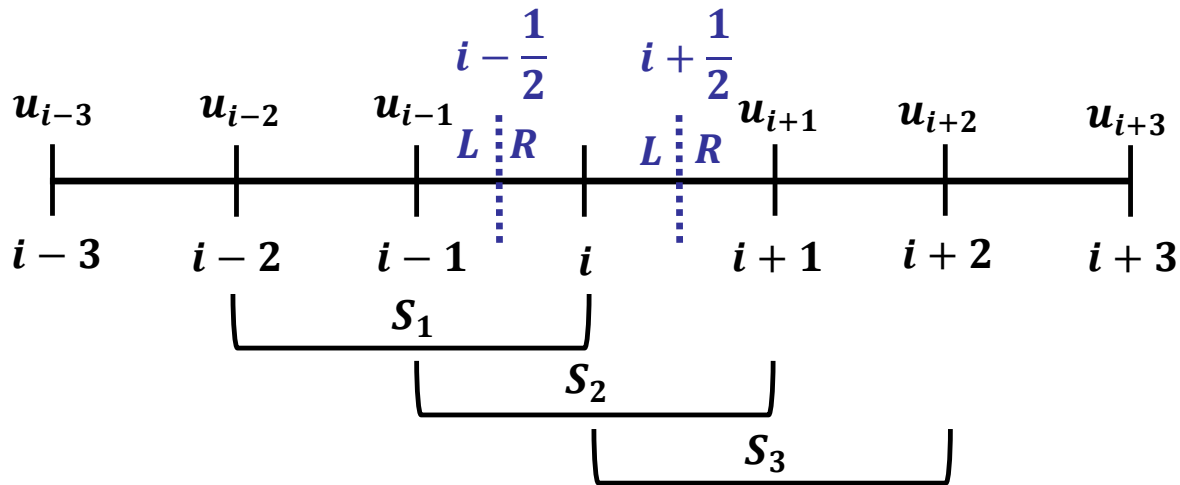
S is the maximum of the eigenvalues

$$\lambda = [u + a, u, u, u - a]$$

Taking a local maximum gives the local Lax-Friedrich flux splitting

Fluxes need to be reconstructed at each cell's left and right interface

- Builds upon Essentially Non-Oscillatory (ENO) schemes developed by Harten et. al. [1]
 - ENO reconstruction uses the smoothest stencil among a set of selected stencils that include a given cell
 - Smoothness indicator is used to determine stencil to be used
 - A reconstruction polynomial is built using the single smoothest stencil of k^{th} order



$$S_1 = [i - 2, i - 1, i] \quad S_2 = [i - 1, i, i + 1] \quad S_3 = [i, i + 1, i + 2]$$

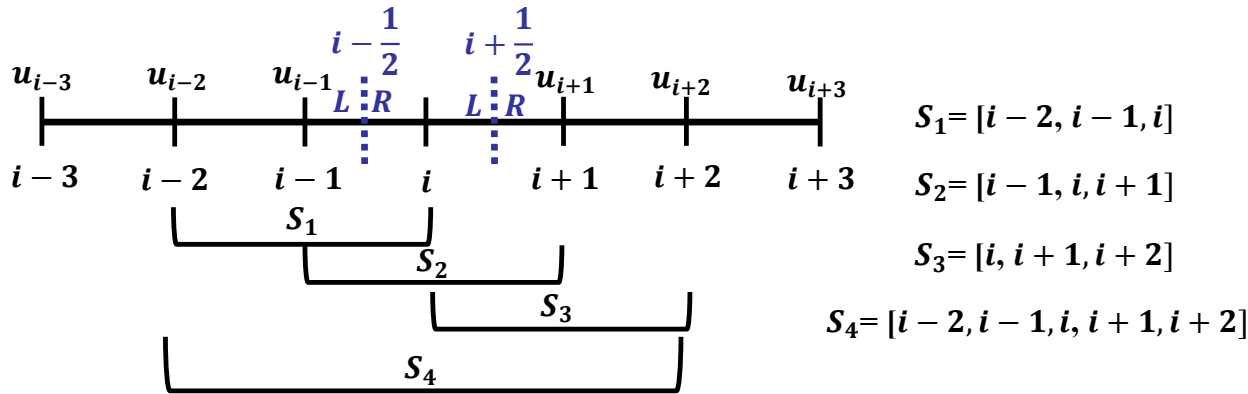
$$u_{i+\frac{1}{2}}^{(1)L} = \frac{1}{3}u_{i-2} - \frac{7}{6}u_{i-1} + \frac{11}{6}u_i$$

$$u_{i+\frac{1}{2}}^{(2)L} = -\frac{1}{6}u_{i-1} + \frac{5}{6}u_i + \frac{1}{3}u_{i+1}$$

$$u_{i+\frac{1}{2}}^{(3)L} = \frac{1}{3}u_i + \frac{5}{6}u_{i+1} - \frac{1}{6}u_{i+2}$$

Third order accurate

- Weighted Essentially Non-Oscillatory (WENO) reconstruction uses a convex combination of all the selected stencils (Jiang, Shu) [2]
 - Weights are determined based local smoothness of the stencil such that:
 - Reconstruction polynomial of $2k^{\text{th}}-1$ order is achieved in smooth regions
 - Reverts to k^{th} order ENO reconstruction near discontinuities



$$u_{i+\frac{1}{2}}^{(1)L} = \frac{1}{3}u_{i-2} - \frac{7}{6}u_{i-1} + \frac{11}{6}u_i$$

$$u_{i+\frac{1}{2}}^{(2)L} = -\frac{1}{6}u_{i-1} + \frac{5}{6}u_i + \frac{1}{3}u_{i+1}$$

$$u_{i+\frac{1}{2}}^{(3)L} = \frac{1}{3}u_i + \frac{5}{6}u_{i+1} - \frac{1}{6}u_{i+2}$$

$$u_{i+\frac{1}{2}}^L = w_1 u_{i+\frac{1}{2}}^{(1)L} + w_2 u_{i+\frac{1}{2}}^{(2)L} + w_3 u_{i+\frac{1}{2}}^{(3)L}$$

5th order accurate if all stencils are smooth

$$\beta_1 = \frac{13}{12}(u_{i-2} - 2u_{i-1} + u_i)^2 + \frac{1}{4}(u_{i-2} - 4u_{i-1} + 3u_i)^2$$

$$\beta_2 = \frac{13}{12}(u_{i-1} - 2u_i + u_{i+1})^2 + \frac{1}{4}(u_{i+1} - u_{i-1})^2$$

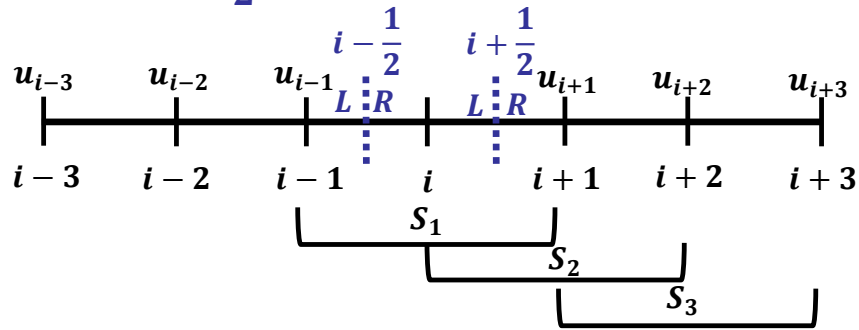
$$\beta_3 = \frac{13}{12}(u_i - 2u_{i+1} + u_{i+2})^2 + \frac{1}{4}(3u_i - 4u_{i+1} + u_{i+2})^2$$

$$\alpha_k = \frac{\gamma_k}{(\beta_k + \epsilon)^2} \quad \text{where } \epsilon \text{ is small to avoid division by zero}$$

$$\gamma_1 = \frac{1}{10} \quad \gamma_2 = \frac{3}{5} \quad \gamma_3 = \frac{3}{10}$$

$$w_k = \frac{\alpha_k}{\sum_{k=1}^3 \alpha_k}$$

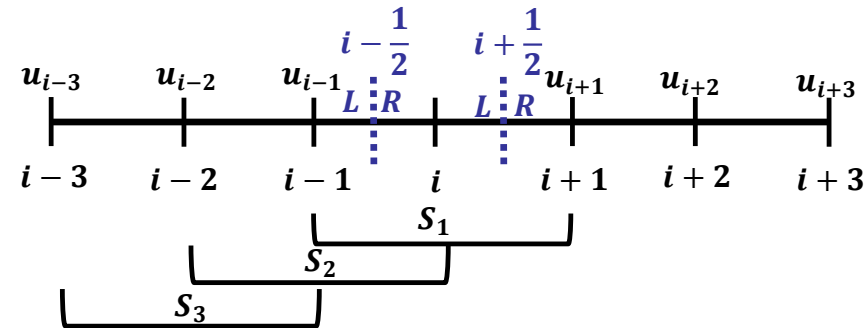
- L reconstruction will have 1 more point left of the interface
- R reconstruction will have 1 more point right of the interface
- For $u_{i+\frac{1}{2}}^{(k)R}$ the stencil needs to be shifted one cell to the right
- For $u_{i-\frac{1}{2}}^{(k)L}$ the stencil needs to be shifted one cell to the left



$$u_{i+\frac{1}{2}}^{(1)R} = -\frac{1}{6}u_{i-1} + \frac{5}{6}u_i + \frac{1}{3}u_{i+1}$$

$$u_{i+\frac{1}{2}}^{(2)R} = \frac{1}{3}u_i + \frac{5}{6}u_{i+1} - \frac{1}{6}u_{i+2}$$

$$u_{i+\frac{1}{2}}^{(3)R} = \frac{1}{3}u_{i+1} - \frac{7}{6}u_{i+2} + \frac{11}{6}u_{i+3}$$



$$u_{i-\frac{1}{2}}^{(1)L} = -\frac{1}{6}u_{i+1} + \frac{5}{6}u_i + \frac{1}{3}u_{i-1}$$

$$u_{i-\frac{1}{2}}^{(2)L} = \frac{1}{3}u_i + \frac{5}{6}u_{i-1} - \frac{1}{6}u_{i-2}$$

$$u_{i-\frac{1}{2}}^{(3)L} = \frac{1}{3}u_{i-1} - \frac{7}{6}u_{i-2} + \frac{11}{6}u_{i-3}$$

- In literature, the coefficients for the reconstruction polynomials may be presented differently
 - Finding a Lagrange interpolating polynomial for each stencil and evaluating at $i+1/2$ for uniform grid spacing, we can obtain

$$\mathbf{u}_{i+\frac{1}{2}}^{(1)L} = \frac{3}{8}\mathbf{u}_{i-2} - \frac{5}{8}\mathbf{u}_{i-1} + \frac{15}{8}\mathbf{u}_i \quad \mathbf{u}_{i+\frac{1}{2}}^{(2)L} = -\frac{1}{8}\mathbf{u}_{i-1} + \frac{3}{4}\mathbf{u}_i + \frac{3}{8}\mathbf{u}_{i+1} \quad \mathbf{u}_{i+\frac{1}{2}}^{(3)L} = \frac{3}{8}\mathbf{u}_i + \frac{3}{4}\mathbf{u}_{i+1} - \frac{1}{8}\mathbf{u}_{i+2}$$

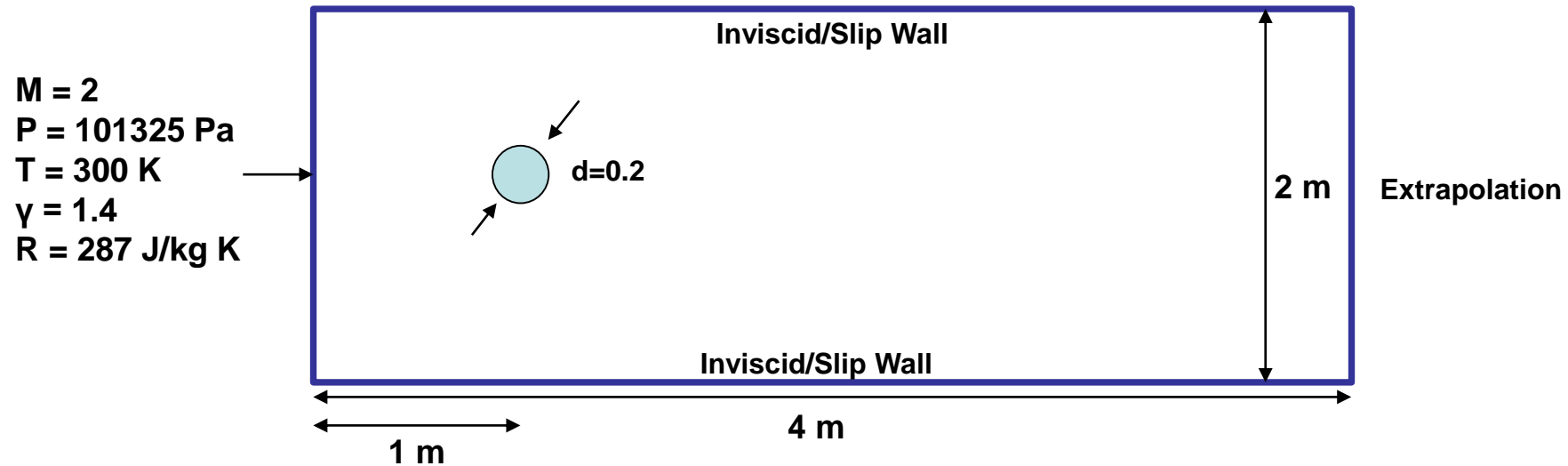
$$\text{with } \gamma_1 = \frac{1}{16}, \gamma_2 = \frac{5}{8} \text{ and } \gamma_3 = \frac{5}{16}$$

- Taking the quadratic $P(s) = as^2 + bs + c$ where $s = (x - x_i)$ and averaging over the cell, we can find a, b, and c to satisfy

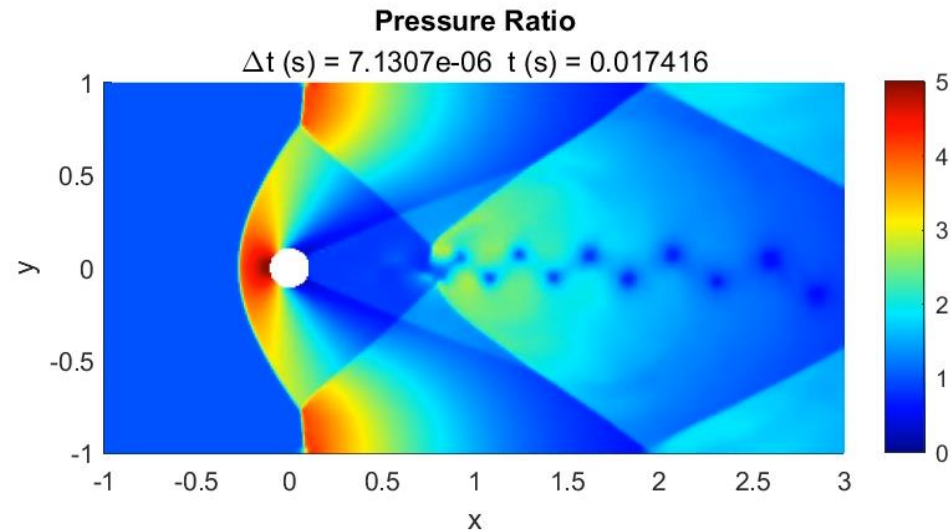
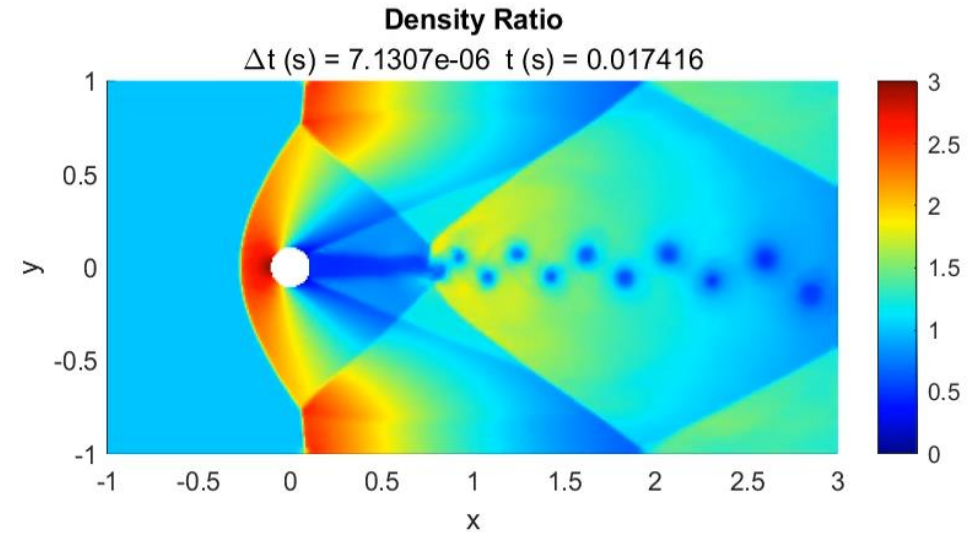
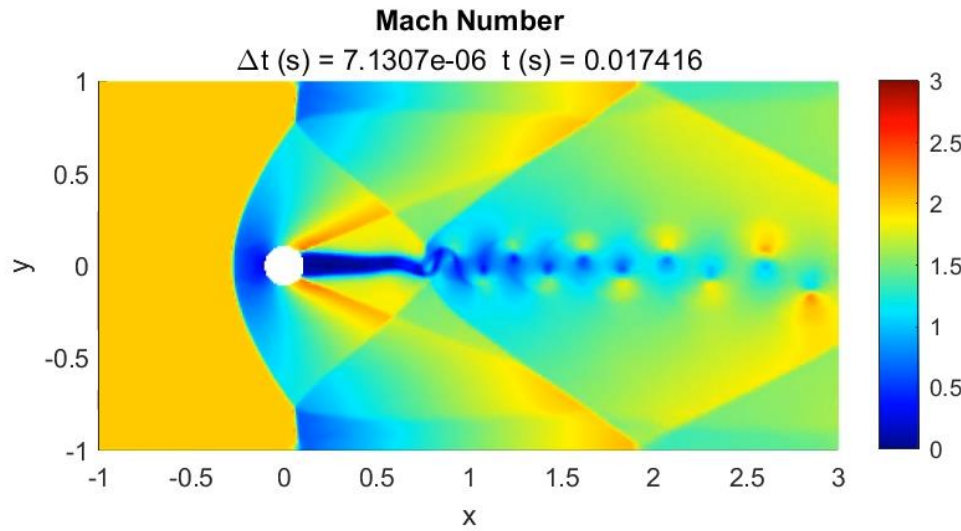
$$\bar{\mathbf{u}}_{i-1} = \int_{-\frac{3\Delta x}{2}}^{-\frac{\Delta x}{2}} P(s) ds \quad \bar{\mathbf{u}}_i = \int_{-\frac{\Delta x}{2}}^{\frac{\Delta x}{2}} P(s) ds \quad \bar{\mathbf{u}}_{i+1} = \int_{\frac{\Delta x}{2}}^{\frac{3\Delta x}{2}} P(s) ds$$

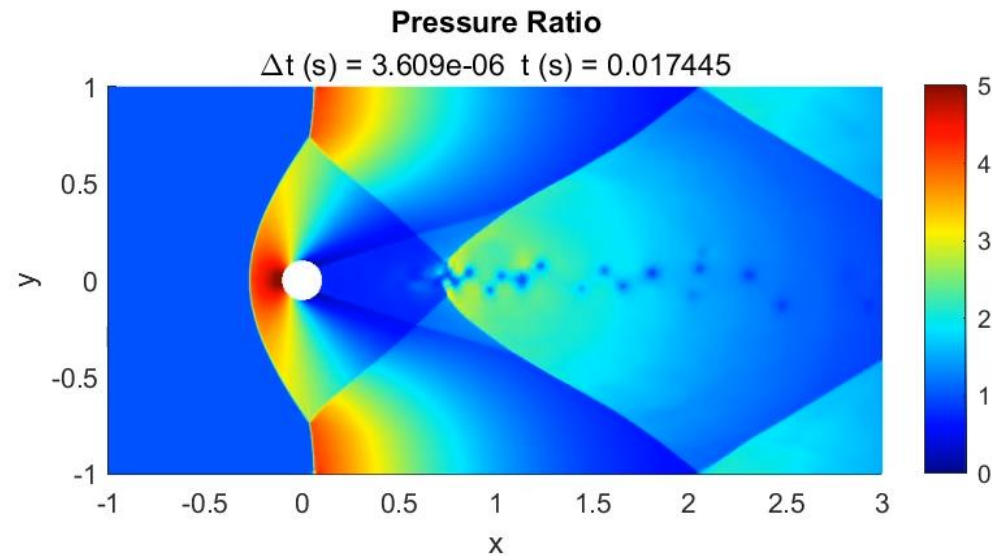
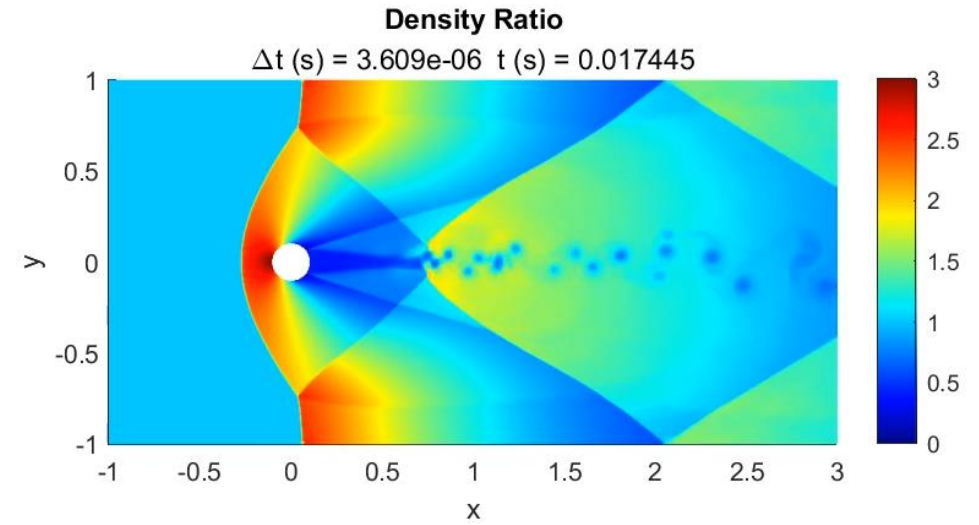
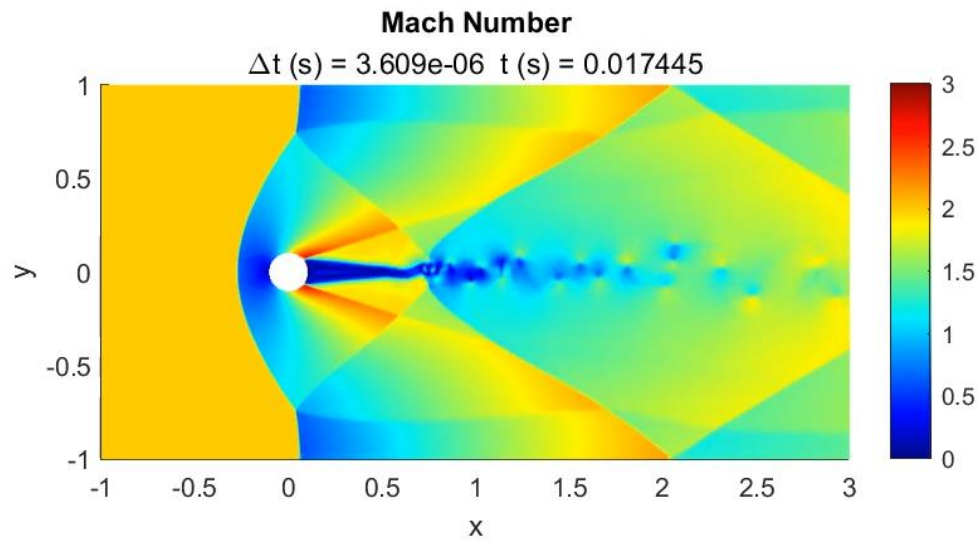
$$\bar{\mathbf{u}}_{i+\frac{1}{2}}^{(1)L} = \frac{1}{3}\mathbf{u}_{i-2} - \frac{7}{6}\mathbf{u}_{i-1} + \frac{11}{6}\mathbf{u}_i \quad \bar{\mathbf{u}}_{i+\frac{1}{2}}^{(2)L} = -\frac{1}{6}\mathbf{u}_{i-1} + \frac{5}{6}\mathbf{u}_i + \frac{1}{3}\mathbf{u}_{i+1} \quad \bar{\mathbf{u}}_{i+\frac{1}{2}}^{(3)L} = \frac{1}{3}\mathbf{u}_i + \frac{5}{6}\mathbf{u}_{i+1} - \frac{1}{6}\mathbf{u}_{i+2}$$

- Test Problem 1
- Domain initialized using inlet conditions
- 400x200 grid points
- 800x400 grid points



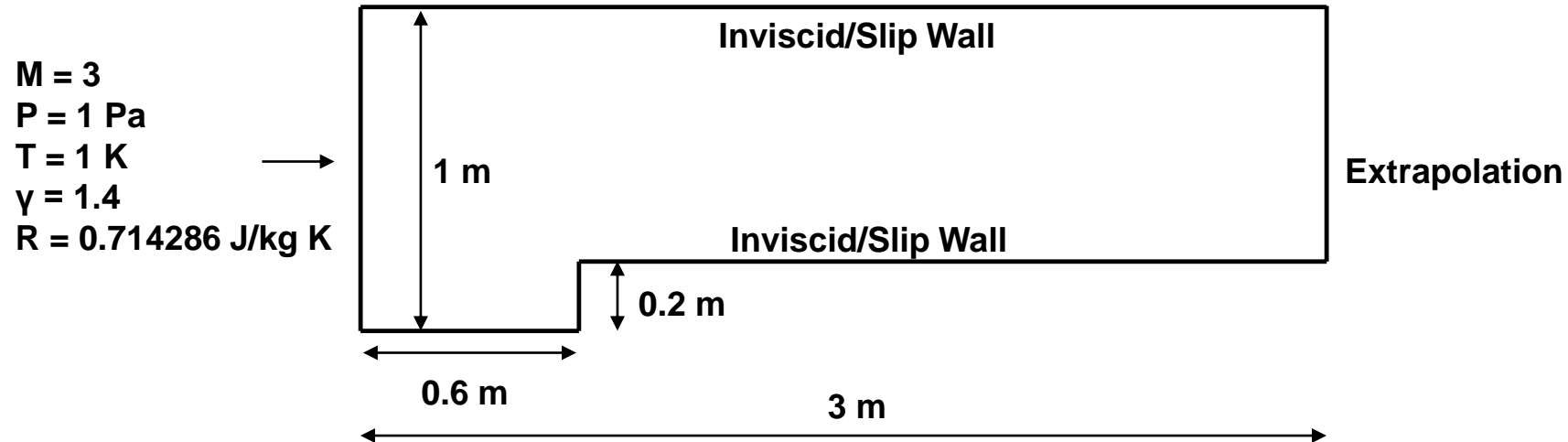
Supersonic Flow over Cylinder (400x200 Grid)

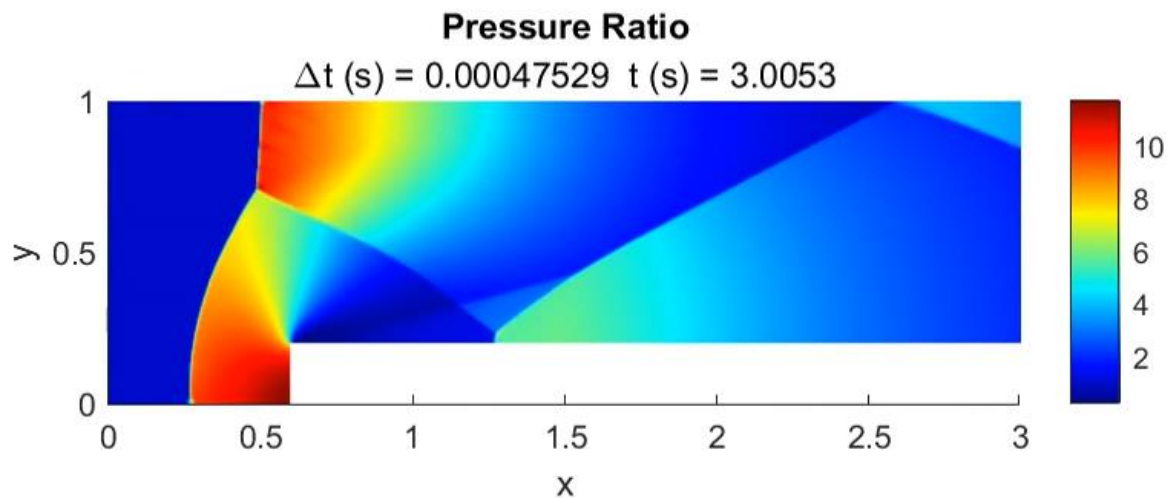
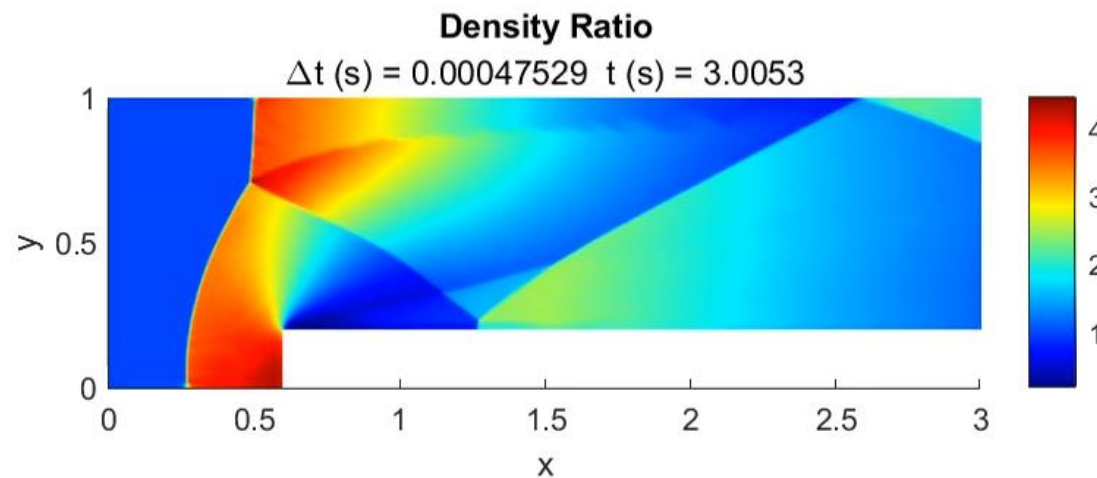
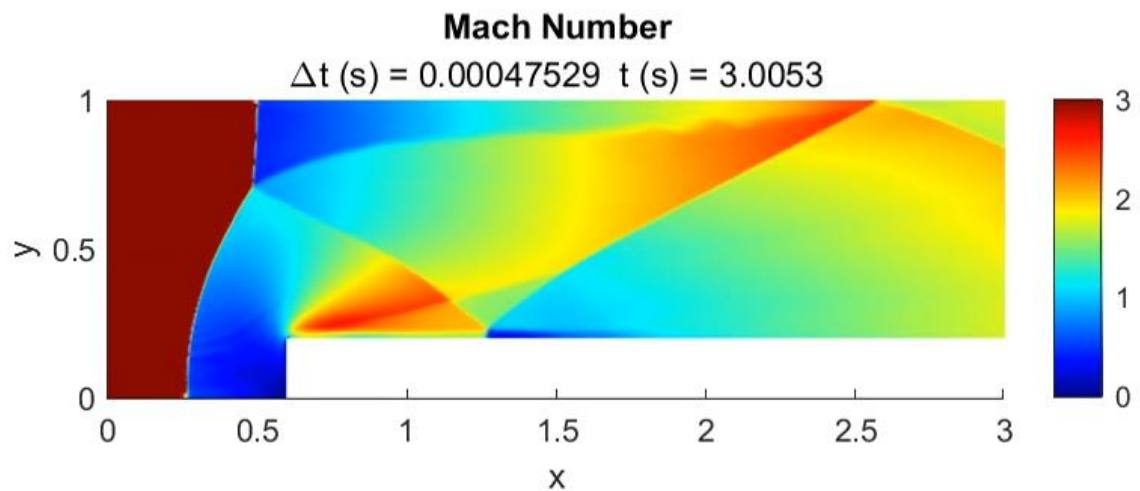




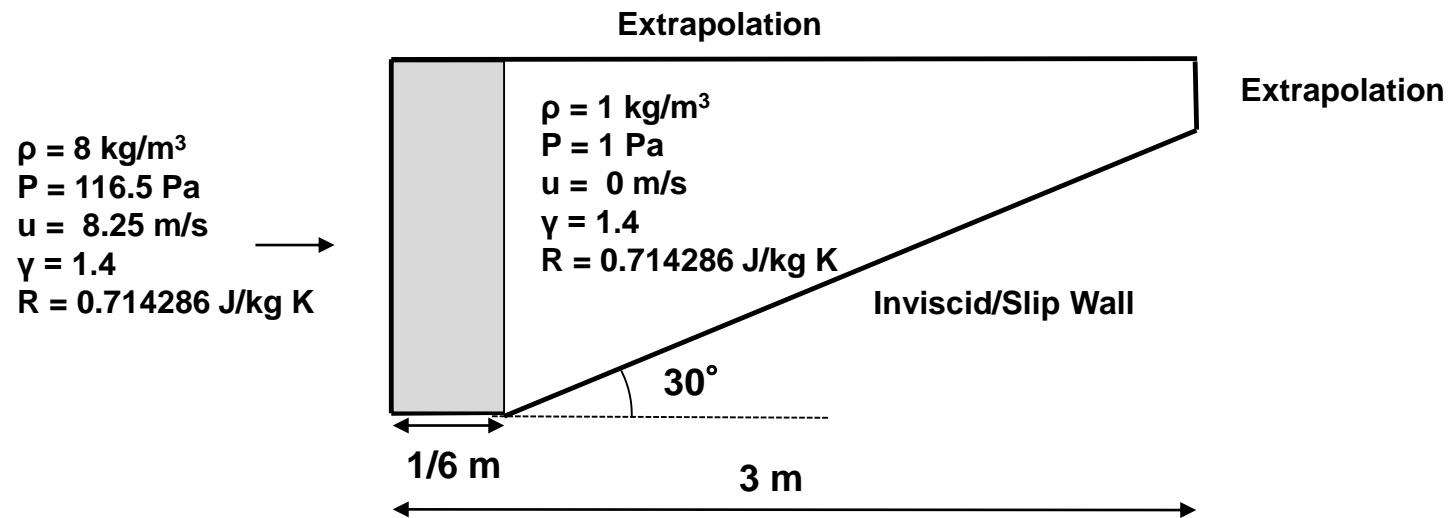
Forward Facing Step

- Test Problem 2
- Domain initialized using inlet conditions
- 600 x 200 grid points

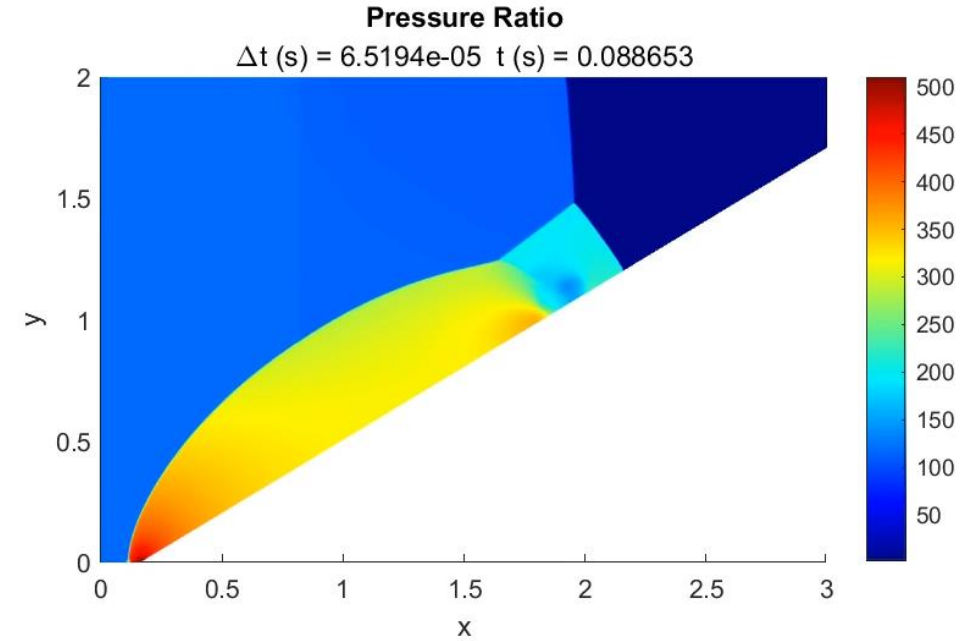
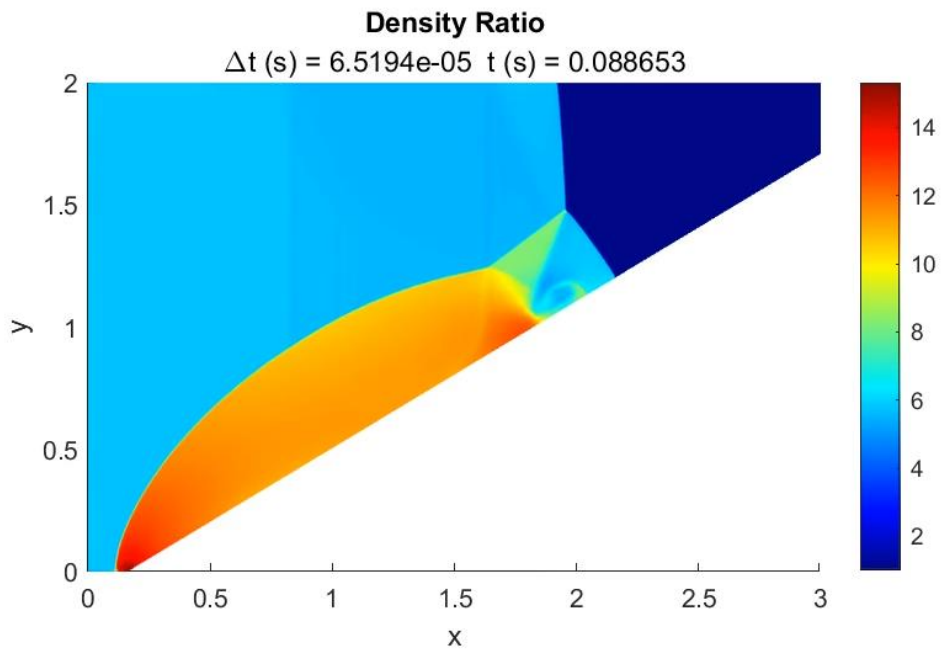




- Test Problem 3
- Grid points $x < 1/6$ m are initialized to give Mach 10 moving shock wave
- $dx = 0.003$



- Test Problem 3
- Grid points $x < 1/6$ m are initialized to give Mach 10 moving shock wave
- $\Delta x = 0.003$





Conclusions and Future Work



- Successfully developed a solver for the Euler Equations using the WENO formulation
 - “Prototype code” for future development
 - Many lessons learned about the WENO method while developing the solver
 - WENO polynomials
 - Nonlinear weights
 - Smoothness indicator
 - Riemann solvers and flux splitting
- Obtained good agreement with test cases
- Find use cases in LSP work
- Future Work
 - Create 3D and axisymmetric solver using lessons learned
 - Utilize GPU computing

References

1. Harten, A., Engquist, B., Osher, S., & Chakravarthy, S.R. (1987). Uniformly high order accurate essentially non-oscillatory schemes, 111. *Journal of Computational Physics*, 71, 231-303.
2. Jiang, G., & Shu, C. (1995). Efficient Implementation of Weighted ENO Schemes. *Journal of Computational Physics*, 126, 202-228.
3. Zahran Y. (2017) Weighted non-oscillatory (WENO) methods for solving hyperbolic conservation laws. Lap Lambert Academic Publishing
4. Yao G. (2018) Immersed Boundary Method for CFD: Focusing on its implementation Second Edition
5. Vázquez-Cendón E. (2011) Lecture Notes on Numerical Methods for Hyperbolic Equations: Short Course Book
6. Hesthaven J. (2018) Numerical Methods for Conservation Laws: From Analysis to Algorithms, Society of Industrial and Applied Mathematics